

**Showcasing research from the laboratories of Professor Shouwei Yin, School of Food Science and Engineering, South China University of Technology, Guangzhou, China and Professor To Ngai, Department of Chemistry, The Chinese University of Hong Kong, Hong Kong, China.**

Growth of Au nanoparticles on phosphorylated zein protein particles for use as biomimetic catalysts for cascade reactions at the oil-water interface

We reported the use of smart protein nanoparticles to anchor artificial enzymes (Au NCs), combined with glucose oxidase (GOx) of the aqueous phase, for realizing a Pickering interfacial catalysis (PIC) cascade reaction, which could successfully recover the catalyst and separate the product by simply adjusting the pH. The results highlighted the preliminary applications of artificial enzymes and bio-enzymes in a one-pot cascade PIC.

### As featured in:



See Shouwei Yin, To Ngai *et al.*, *Chem. Sci.*, 2021, **12**, 3885.

Cite this: *Chem. Sci.*, 2021, 12, 3885

All publication charges for this article have been paid for by the Royal Society of Chemistry

# Growth of Au nanoparticles on phosphorylated zein protein particles for use as biomimetic catalysts for cascade reactions at the oil–water interface†

Yongkang Xi,<sup>‡a</sup> Bo Liu,<sup>‡a</sup> Shuxin Wang,<sup>a</sup> Xiaonan Huang,<sup>a</sup> Hang Jiang,<sup>b</sup> Shouwei Yin,<sup>id</sup>\*<sup>acd</sup> To Ngai,<sup>id</sup>\*<sup>b</sup> and Xiaoquan Yang<sup>a</sup>

Chemo-enzymatic cascade processes are invaluable due to their ability to rapidly construct high-value products from available feedstock chemicals in a one-pot relay manner. However, they have proven to be challenging because of the mutual inactivation of both catalysts. A conceptually novel strategy based on Pickering interfacial catalysis (PIC) is proposed here to address this challenge. This study aimed to construct a protein-stabilized Pickering system for biphasic cascade catalysis, enabled by phosphorylated zein nanoparticles (ZCPOPs) immobilized in gold nanoparticles (Au NCs). Ultra-small Au NCs, 1–2 nm in diameter, were integrated into ZCPOPs at room temperature. Then, the as-synthesized ZCPOPs–Au NCs were used to stabilize the oil-in-water (o/w) Pickering emulsion. Besides their excellent catalytic activity and recycling ability in a variety of oil phases, ZCPOPs–Au NCs possess unpredictable catalytic activity and exhibit mimicking properties of horseradish peroxidase. Particularly, the cascade reaction is well achieved using a metal catalyst and a biocatalyst at the oil–water interface. The result showed that such a combination of chemo- and biocatalysis improved the catalytic yield more than two times compared with that of sole metal catalysis. This study opened a new avenue to design nanomaterials using the combination of chemo- and biocatalysis in a Pickering emulsion system for multistep syntheses.

Received 5th December 2020  
Accepted 16th February 2021

DOI: 10.1039/d0sc06649d

rsc.li/chemical-science

## Introduction

Cascade reactions enable two or more steps in a one-pot reaction without isolation of intermediates to bypass tedious workups, degradation of the intermediates, and the cost and time associated with pharmaceutical and chemical manufacturing.<sup>1,2</sup> In particular, chemo-enzymatic cascade reactions represent an emerging strategy in chemical synthesis, and enable novel synthetic pathways that combine the reactivity of chemical catalysts with the selectivity of enzymes, and create useful one-pot transformations unattainable with biocatalysts or chemocatalysts alone.<sup>1,3,4</sup> However, the major challenges that need to be addressed are still compatibility problems and

mutual inactivation upon combining chemocatalysts with biocatalysts.<sup>1,2,5</sup> So far, a majority of the current reported strategies relied on homogeneous reactions where toxic co-solvents and phase-transferable reagents were routinely used to increase compatibility.<sup>6–8</sup> A biphasic reaction offers several advantages over a homogeneous reaction, such as environment-friendly processes, easy isolation, and separation of the catalyst from the reaction mixture, thus reducing downstream costs.<sup>9</sup> However, very few examples have been reported for biphasic reactions, primarily due to limitations related to the small organic/aqueous interfacial area.<sup>10–12</sup>

Pickering interfacial catalysis (PIC) stabilized using catalytically active micro-/nanoparticles has been developed for the design of efficient biphasic catalytic reactions owing to its advantages including no diffusion-related limitations in liquid–liquid reactions, large interfacial areas, and upgradation of ecological benefits of the reaction system.<sup>10,13,14</sup> In 2010, Resasco and co-workers published the first example of PIC in which efficient biofuel-upgrade reactions were realized using actively palladium–carbon nanotube hybrid nanoparticles as emulsifiers.<sup>15</sup>; researchers reported a variety of PIC examples for oxidation,<sup>16</sup> reduction,<sup>17</sup> and hydrogenolysis reactions.<sup>18</sup> Recently, the PIC concept evolved into Pickering interfacial biocatalysis (PIB), in which biohybrid catalyst particles were

<sup>a</sup>Research and Development Centre of Food Proteins, School of Food Science and Engineering, Guangdong Province Key Laboratory for Green Processing of Natural Products Safety, South China University of Technology, Guangzhou, 510640, P. R. China. E-mail: feysw@scut.edu.cn

<sup>b</sup>Department of Chemistry, The Chinese University of Hong Kong, Shatin, NT, Hong Kong. E-mail: tongai@cuhk.edu.hk

<sup>c</sup>Sino-Singapore International Joint Research Institute, Guangzhou 510640, P. R. China

<sup>d</sup>Research Institute for Food Nutrition and Human Health, Guangzhou, P. R. China

† Electronic supplementary information (ESI) available: Experimental details and results. See DOI: 10.1039/d0sc06649d

‡ The authors contributed equally to this work.



designed for carrying out PIC.<sup>19,20</sup> In a pioneering study, Wu and co-workers synthesized robust and recyclable enzyme-polymer conjugates by “grafting-from” atom-transfer radical polymerization as Pickering emulsifiers, and constructed for the first time a robust carrier-free biocatalyst-stabilized PIB as well as enzyme-enzyme cascade PIB.<sup>12</sup> The as-prepared conjugation is a generic and robust method for PIB, and this strategy promotes not only reaction efficiency but also biocatalyst recyclability and usability after operation. In general, the stability and activity of natural enzymes are compromised due to exposure to the reaction interface. Artificial enzymes with enzyme-mimicking activities are currently a hot research topic because of their obvious advantages, such as similar enzyme catalytic activities, facile preparation, low cost, and superior stability, compared with natural enzymes.<sup>21–24</sup> As such, incorporating artificial enzymes instead of natural enzymes into one-pot relay PIC can make full use of their advantages and complement each other, allowing for the direct transformation of available feedstock chemicals to high-value products.<sup>25,26</sup> However, Pickering emulsion-based metal-enzyme cascade reactions have not been explored to date.

Recently, proteins have been found to have emerging applications in designing protein-based materials, resolving a vast array of technical challenges.<sup>27</sup> For example, protein-based materials were explored to design new catalysts with desirable activity and showed many advantages, including biocompatibility, high water dispersion, and ease of further conjugation, which were not accessible for conventional inorganic nanoparticles or natural organics.<sup>28,29</sup> In particular, the amphiphilic nature of proteins allows its supported catalyst to anchor on the interface, thereby affecting the catalytic efficiency.<sup>30</sup>

This study reported the use of smart protein nanoparticles to anchor artificial enzymes (Au NCs), combined with glucose oxidase (GOx) of the aqueous phase, for realizing a PIC cascade reaction. Specifically, a Au/ZCPOP catalyst (ZCPOPs–Au NC) was developed by growing Au NCs *in situ* onto ZCPOPs. Then, the as-prepared nanoparticles were used for formulating a Pickering emulsion platform for interfacial catalysis. Finally, one unanticipated finding was that the ZCPOPs–Au NC exhibited mimicking properties of horseradish peroxidase (HRP). Particularly, the cascade reaction was well achieved using the ZCPOPs–Au NC and GOx as the catalyst to produce methyl phenyl sulfoxide (intermediate for medicine, pesticides, and expensive materials) for the first time.

## Results and discussion

“Smart” protein nanoparticles were prepared by a two-step procedure (Fig. 1a). The nanoparticles were synthesized by the reaction of a POCl<sub>3</sub> with amino groups of zein proteins, followed by zein self-assembly. The obtained ZCPOPs exhibited the characteristic infrared absorption of PO<sub>4</sub><sup>3–</sup> in the Fourier transform infrared (FTIR) spectrum (Fig. S1a†), demonstrating their successful graft of zein.<sup>31</sup> X-ray photoelectron spectroscopy (XPS) data further supported this result. As shown in Fig. S1b (in the ESI)†, after grafting PO<sub>4</sub><sup>3–</sup>, the N 1s XPS peaks for ZCPOPs were shifted toward a lower binding energy (~0.5 eV), because the electron donation by –P in PO<sub>4</sub><sup>3–</sup> could increase the electron

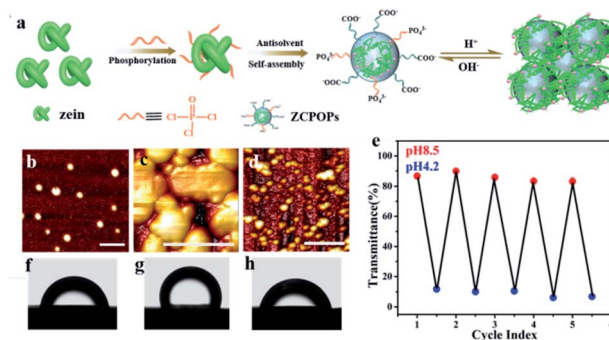


Fig. 1 (a) Schematic illustration of the ZCPOP strategy. AFM image and contact angles of ZCPOPs at pH 8.5 (b and f), pH 4.2 (c and g) and 6 cycles (d and h) of switching the pH value between 8.5 and 4.2, with a scale bar of 1.0  $\mu\text{m}$  (b–d). (e) Reversible transmittance changes of ZCPOP solution upon cycling between pH 8.5 and pH 4.2.

density of N atoms. These results confirmed the formation of phosphorylated zein. In brief, per mol zein gave an average value of 7.4 mol phosphate groups according to ICP-AES.

Following the spectroscopic study, reversible pH-responsive association–disassociation of ZCPOPs was investigated. ZCPOPs were spherical with diameters of 60–100 nm at pH 8.5 and were structurally stable at room temperature over several days (Fig. 1b). The nanoparticles evolved into a 2  $\mu\text{m}$  colloidal architecture (Fig. S2a in the ESI†) when the pH shifted to 4.2, and they formed a cluster-like colloidal architecture as the solutions were further acidized (Fig. 1c; see also Fig. S2b†), and precipitated finally upon storage (Fig. S2c†). Interestingly, this association was fully reversible when the pH was adjusted back to 8.5 (Fig. 1d and e). Fig. 1d shows that the morphology of ZCPOPs remained unaffected even after six cycles. In particular, the dilution made the as-mentioned colloidal architecture at pH 4.2 return to uniform nanoparticles in the range of 40–80 nm (Fig. S2d–f†), suggesting that they flocculated but did not merge or coalescence during acidification. One also has to consider wettability because it is an important factor in emulsification. As shown in Fig. 1f–h, the three-phase contact angle of ZCPOPs verified that its wettability had good responsiveness. Based on these excellent properties, the pH-responsive performance of Pickering emulsion stabilized ZCPOPs was examined. The as-prepared Pickering emulsion was stable over at least 24 h (Fig. S3†). This emulsion could be reversibly turned on and off over 10 cycles by simply adjusting the pH value, and this pH-responsive performance was robust and universally applicable to all oil phases (interface tension was distributed from 1.8 to 51.1  $\text{mN m}^{-1}$ ), suggesting that the strategy was versatile (Table S1 and Fig. S4–S7†).

Based on the aforementioned observations, ZCPOP-stabilized emulsions were used as a platform for creating efficiently recyclable catalytic systems. To this end, a Au/ZCPOP catalyst (ZCPOPs–Au) was prepared by growing Au NCs *in situ* onto ZCPOPs. Then, the as-prepared nanoparticles were used to construct a Pickering emulsion for interfacial catalysis. Transmission electron microscopy (TEM) and scanning electron microscopy (SEM) micrographs reflected that the particles of



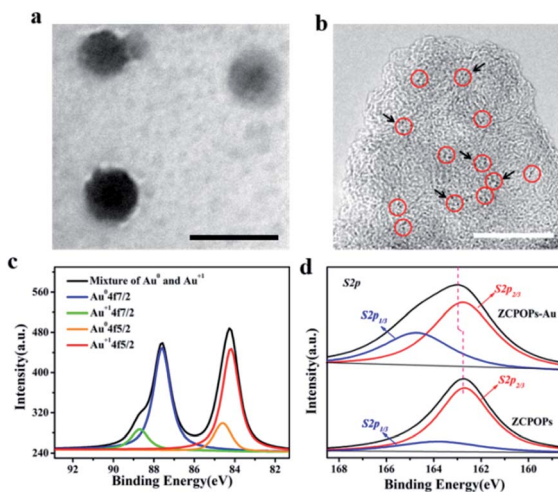


Fig. 2 Size of the ZCPOPs-Au NCs. TEM images at pH 8.5 (a and b) with scale bars of 100 nm and 25 nm, respectively. XPS spectra of the ZCPOPs-Au NCs (c and d).

ZCPOPs-Au adopted a solid spherical morphology with diameters of 60–80 nm (Fig. 2a), and the Au NCs content of ZCPOPs-Au was 0.71 wt% determined by ICP-AES. High-resolution transmission electron microscopy (HR-TEM) analysis found that the Au NCs in the ZCPOPs-Au (Fig. 2b) samples were distributed evenly on the surface of the particles with the average size of 1–2 nm. The absence of a peak at 519 nm in the UV-vis spectra of ZCPOPs-Au NCs further confirmed the *in situ* formation of Au NCs (Fig. S8†).<sup>32</sup> The Au state was further characterized by XPS, suggesting that Au<sup>3+</sup> precursors were fully reduced to yield Au NCs (Fig. 2c).<sup>33,34</sup> High-resolution XPS was utilized to provide a deep understanding. As is known, the coordination of Au NCs and thiols leads to charge transfer, and more attention was paid to the XPS peak shift of S. After grafting Au NCs, both S 2p<sub>1/2</sub> and S 2p<sub>3/2</sub> peaks were transferred to a higher binding energy (~0.2 eV) (Fig. 2d), which verified that the electron density of S in the ZCPOPs-Au NCs was reduced concomitantly. Based on these findings, a mechanism for the formation of ZCPOPs-Au NCs was proposed (Fig. S9†).

Subsequently, shearing the ZCPOPs-Au NC solution with the oil phase at a water/oil volume ratio ( $\phi_w$ ) of 1 : 1 yielded a stable emulsion (Fig. S10a†). The interface architecture of droplets was investigated by forming a hollow microsphere with diameters of 10–50  $\mu$ m to better understand the Au NC behavior anchored at the interface. The granular architecture on the surface of droplets was clearly visible in the SEM images of the partially dried emulsion, which showed a close-packed array of nanoparticles (Fig. S10b and c†). TEM images verified that the interfacial ZCPOPs-Au NC shell consisted of a rough membrane decorated with Au NCs, confirming the formation of the interfacial layer coated with Au NCs (Fig. 3b and c). This was supported by the appearance of the Au signal in the SEM-EDS image (Fig. 3d). In addition, this unusual behavior was further detected using confocal scanning microscopy (CLSM). A green aperture surrounded the oil droplets, confirming that robust Pickering emulsions were formed with ZCPOPs-Au NCs as emulsifiers and potential catalysts (Fig. S10d†).

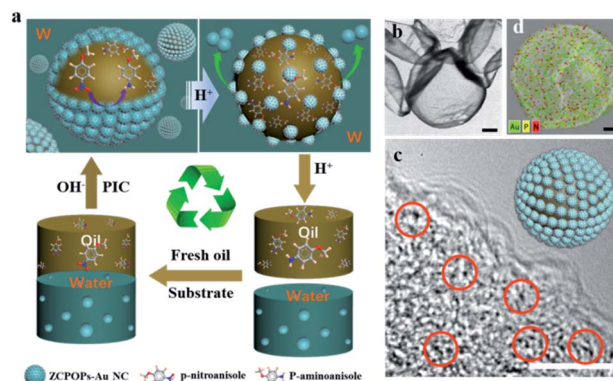


Fig. 3 (a) Schematic illustration of PIC stabilized by ZCPOPs-Au NCs. TEM images (b and c), and SEM-EDS images (d) of pH-responsive Pickering emulsion. The scale bars of b, c and d were 2  $\mu$ m, 5 nm and 2  $\mu$ m, respectively.

The existence of interfacial catalysts facilitated the construction of a Pickering interfacial catalysis (PIC) system. A PIC system was designed and tested using a typical hydrogenation reaction of *p*-nitroanisole in an aqueous/ethyl acetate two-phase system to determine catalytic efficiency, isolation and separability, along with recyclability of the ZCPOPs-Au NCs. The developed ZCPOPs-Au NC-based PIC systems were robust, pH-responsive and highly recyclable, which was highlighted by the high productivity throughout at least eight reaction cycles with all conversions over 99% (Fig. S11†). Recyclable catalysis with different kinds of oil was performed to further justify the high effectiveness of this method. Emulsion catalysis was robustly extended to other systems such as toluene–water, chloroform–water, and benzene–water systems (Fig. S12–S14†).

This protein-based PIC system was explored as an unprecedented platform for multistep cascade reactions to circumvent the isolation and purification of intermediates. In brief, glucose oxidase (GOx) was selected for enzymatically producing hydrogen peroxide which was used by a second ZCPOPs-Au NC (HRP-mimicking activity). This strategy possesses an excellent ecological profile. To prove this, we investigated first the peroxidase-like catalytic activity of ZCPOPs-Au NCs. Typically, TMB was chosen as a substrate to examine the peroxidase-like catalytic activity of ZCPOPs-Au NCs (Fig. 4a).<sup>35–37</sup> As shown in Fig. 4b, different pH values of ZCPOPs-Au NCs were associated with different peroxidase-like activities, and pH 3 showed the best conditions for catalysis. Furthermore, the reaction solution with various concentrations of ZCPOPs-Au NCs showed intense characteristic absorbance of TMB\*, proving that ZCPOPs-Au NCs had intrinsic peroxidase-like activities (Fig. 4c). To further consolidate the aforementioned results, the reaction was monitored in a time-dependent manner, and the reaction catalyzed by ZCPOPs-Au NCs had a good reaction rate (Fig. 4d). To further validate it, the peroxidase-like activities of ZCPOPs-Au NCs were tested using other chromogenic reagents (*i.e.*, ABTS and OPD) as substrates. The solution showed detectable absorption peaks at 416 and 450 nm in the absence of ZCPOPs-Au NCs (Fig. 4e), demonstrating that they had excellent peroxidase-like activities.



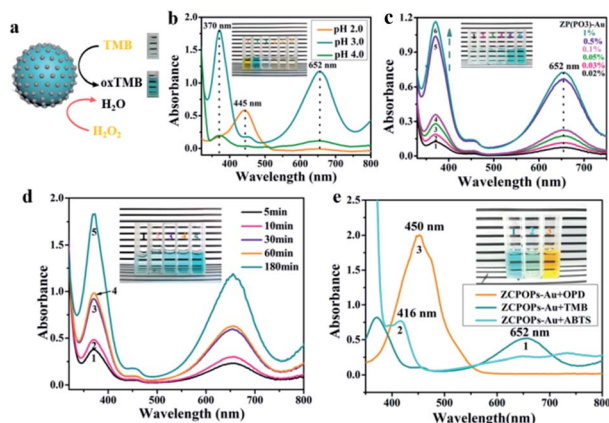


Fig. 4 HRP-mimicking properties of ZCPOPs-Au NCs. (a) Schematic illustration of PIC systems with ZCPOPs-Au NC as the emulsifier and catalyst. (b) pH-dependent HRP-mimicking properties of ZCPOPs-Au NCs. (c) Absorbance curves of the concentration-dependent activities of ZCPOPs-Au NCs. (d) Time-dependent absorbance for the ZCPOPs-Au NCs. (e) Absorbance curves of TMB, ABTS, and OPD oxidation by H<sub>2</sub>O<sub>2</sub> in the presence of ZCPOPs-Au NCs.

ZCPOPs-Au NCs were then used to catalyze a two-step cascade reaction (Fig. 5a) in an o/w Pickering emulsion in which the enzyme (GOx) was dispersed in the water phase, to

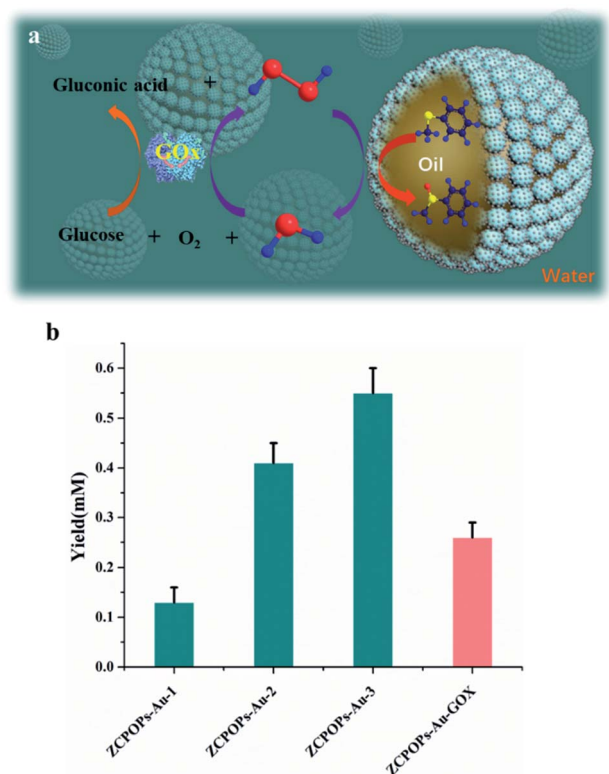


Fig. 5 Cascade reaction of GOx-ZCPOPs-Au NCs. (a) Schematic illustration of the cascade reaction. (b) Activity comparison of ZCPOPs-Au NCs with or without GOx in GOx-Au NC cascade reactions. ZCPOPs-Au-1, ZCPOPs-Au-2, and ZCPOPs-Au-3 contained 80  $\mu$ M, 200  $\mu$ M, and 400  $\mu$ M hydrogen peroxide, respectively.

prepare a valuable intermediate: methyl phenyl sulfoxide. In particular, the productivity calculated from the final products when metal-enzyme cascade catalysis reaction efficiency was applied was significantly improved (Fig. 5b). For example, the metal-enzyme catalysis increased the yield more than two times when compared with sole metal catalysis (80  $\mu$ M hydrogen peroxide added, which was approximately equal to the amount of hydrogen peroxide produced by pristine GOx in solution). Last but not least, the PIC cascade reactions at 2 h gave rise to over 65-fold improvement in catalytic efficiency compared with a two-phase system (Fig. S15†). This improvement might be due to the cascade reaction that promoted GOx to produce more hydrogen peroxide, which in turn increased the yield of methyl phenyl sulfoxide.

In summary, robust protein-stabilized chemo- and bio-catalytic cascade PIC with a recovery catalyst and a separation product was successfully developed *via* adjusting pH. Along with good reusability, the PIC had excellent universality with the oil phase. With this cascade PIC, a continuous process could be designed in which the ZCPOPs-Au NCs with peroxidase-like activity at the interface continuously produced methyl phenyl sulfoxide with hydrogen peroxide as a substrate (product of GOx), and then continuously removed oil-soluble products from the top layer while the reaction continued in the Pickering emulsion. Overall, the results groundbreakingly highlighted the preliminary applications of artificial enzymes and bio-enzymes in one-pot cascade PIC. Furthermore, the key advantage of the vehicles used in the PIC systems was self-assembled protein colloidal particles, which provided the possibility for catalytically producing functional products for the food and medicine industry, with the concept of sustainable and green chemistry. Therefore, this conceptually novel strategy might open impressive avenues to establish green and sustainable PIC platforms.

## Conflicts of interest

There are no conflicts to declare.

## Acknowledgements

This work was financially supported by the Guangdong Special Support Program (2019BT02N112), the Hong Kong Special Administration Region (HKSAR) General Research Fund (CUHK14304619 and 2130642), the 111 Project (B17018), Sino-Singapore International Joint Research Institute (Contract No. 201-A018003), and the Special fund for the Science and Technology Innovation Strategy of Guangdong Province in 2018 (special major programme + task).

## Notes and references

- 1 F. Rudroff, M. D. Mihovilovic, H. Gröger, R. Snajdrova, H. Iding and U. T. Bornscheuer, *Nat. Catal.*, 2018, **1**, 12–22.
- 2 S. Dutta, N. Kumari, S. Dubbu, S. W. Jang, A. Kumar, H. Ohtsu, J. Kim, M. Kawano, S. H. Cho and I. S. Lee, *Angew. Chem., Int. Ed.*, 2020, **59**, 3416–3422.





- 3 S. Wu, Y. Zhou, D. Gerngross, M. Jeschek and T. R. Ward, *Nat. Commun.*, 2019, **10**, 1–10.
- 4 Z. C. Litman, Y. Wang, H. Zhao and J. F. Hartwig, *Nature*, 2018, **560**, 355–359.
- 5 H. Groeger and W. Hummel, *Curr. Opin. Chem. Biol.*, 2014, **19**, 171–179.
- 6 J. H. Sattler, M. Fuchs, K. Tauber, F. G. Mutti, K. Faber, J. Pfeffer, T. Haas and W. Kroutil, *Angew. Chem., Int. Ed.*, 2012, **51**, 9156–9159.
- 7 Y. C. Lee, S. Dutta and K. C. W. Wu, *ChemSusChem*, 2014, **7**, 3241–3246.
- 8 A. Jakoblinnert and D. Rother, *Green Chem.*, 2014, **16**, 3472–3482.
- 9 Y. Huo, H. Zeng and Y. Zhang, *ChemSusChem*, 2016, **9**, 1078–1080.
- 10 M. Pera-Titus, L. Leclercq, J. M. Clacens, F. De Campo and V. Nardello-Rataj, *Angew. Chem., Int. Ed.*, 2015, **54**, 2006–2021.
- 11 O. Wachsen, K. Himmler and B. Cornils, *Catal. Today*, 1998, **42**, 373–379.
- 12 Z. Sun, U. Glebe, H. Charan, A. Böker and C. Wu, *Angew. Chem., Int. Ed.*, 2018, **57**, 13810–13814.
- 13 H. Yang, T. Zhou and W. Zhang, *Angew. Chem., Int. Ed.*, 2013, **52**, 7455–7459.
- 14 L. Qi, Z. Luo and X. Lu, *Green Chem.*, 2019, **21**, 2412–2427.
- 15 S. Crossley, J. Faria, M. Shen and D. E. Resasco, *Science*, 2010, **327**, 68–72.
- 16 J. Zhang, A. Wang, Y. Wang, H. Wang and J. Gui, *Chem. Eng. J.*, 2014, **245**, 65–70.
- 17 X. Xu, Y. Li, Y. Gong, P. Zhang, H. Li and Y. Wang, *J. Am. Chem. Soc.*, 2012, **134**, 16987–16990.
- 18 H. Tan, P. Zhang, L. Wang, D. Yang and K. Zhou, *Chem. Commun.*, 2011, **47**, 11903–11905.
- 19 C. Wu, S. Bai, M. B. Ansorge-Schumacher and D. Wang, *Adv. Mater.*, 2011, **23**, 5694–5699.
- 20 Z. Sun, M. Cai, R. Hübner, M. B. Ansorge-Schumacher and C. Wu, *ChemSusChem*, 2020, **13**, 6523–6527.
- 21 J. Li, J. Huang, Y. Lyu, J. Huang, Y. Jiang, C. Xie and K. Pu, *J. Am. Chem. Soc.*, 2019, **141**, 4073–4079.
- 22 B. Xu, H. Wang, W. Wang, L. Gao, S. Li, X. Pan, H. Wang, H. Yang, X. Meng and Q. Wu, *Angew. Chem., Int. Ed.*, 2019, **58**, 4911–4916.
- 23 K. Fan, J. Xi, L. Fan, P. Wang, C. Zhu, Y. Tang, X. Xu, M. Liang, B. Jiang and X. Yan, *Nat. Commun.*, 2018, **9**, 1–11.
- 24 Y. Lin, J. Ren and X. Qu, *Acc. Chem. Res.*, 2014, **47**, 1097–1105.
- 25 S. Afewerki and A. Cordova, *Chem. Rev.*, 2016, **116**, 13512–13570.
- 26 Z. Du and Z. Shao, *Chem. Soc. Rev.*, 2013, **42**, 1337–1378.
- 27 P. Gupta and K. K. Nayak, *Polym. Eng. Sci.*, 2015, **55**, 485–498.
- 28 J. C. Lewis, *Acc. Chem. Res.*, 2019, **52**, 576–584.
- 29 H. Li, W. Zhu, A. Wan and L. Liu, *Analyst*, 2017, **142**, 567–581.
- 30 Y. Xi, B. Liu, H. Jiang, S. Yin, T. Ngai and X. Yang, *Chem. Sci.*, 2020, **11**, 3797–3803.
- 31 L. Hao, G. Lin, C. Chen, H. Zhou, H. Chen and X. Zhou, *J. Agric. Food Chem.*, 2019, **67**, 9989–9999.
- 32 Y. Liu, L. Liu, M. Yuan and R. Guo, *Colloids Surf., A*, 2013, **417**, 18–25.
- 33 Y. Liu, Q. Yao, X. Wu, T. Chen, Y. Ma, C. N. Ong and J. Xie, *Nanoscale*, 2016, **8**, 10145–10151.
- 34 H. Kawasaki, K. Hamaguchi, I. Osaka and R. Arakawa, *Adv. Funct. Mater.*, 2011, **21**, 3508–3515.
- 35 Y. Zhao, Y. Huang, H. Zhu, Q. Zhu and Y. Xia, *J. Am. Chem. Soc.*, 2016, **138**, 16645–16654.
- 36 Y. Huang, M. Zhao, S. Han, Z. Lai, J. Yang, C. Tan, Q. Ma, Q. Lu, J. Chen and X. Zhang, *Adv. Mater.*, 2017, **29**, 1700102.
- 37 H. Zhang, X. Liang, L. Han and F. Li, *Small*, 2018, **14**, 1803256.

